

## Observation of the Discrete Electron Energy States of an Individual Nanometer-Size Supported Gold Cluster

M. E. Lin,<sup>(1)</sup> R. P. Andres,<sup>(2)</sup> and R. Reifenberger<sup>(1)</sup>

<sup>(1)</sup>*Department of Physics, Purdue University, West Lafayette, Indiana 47907*

<sup>(2)</sup>*School of Chemical Engineering, Purdue University, West Lafayette, Indiana 47907*

(Received 5 November 1990)

The electron energy distribution from a single 1-nm-diam Au cluster supported on a W(110) field-emission tip has been studied using energy-resolved field-emission microscopy. The emitted electrons provide information on the quantum electron energy states of the supported cluster and demonstrate that these states survive after deposition onto a substrate. A model that accounts for the salient features in the energy distribution is described.

PACS numbers: 79.70.+q, 03.65.-w, 36.40.+d, 61.16.Di

Cluster-beam studies have revealed anomalous features in the abundance of clusters produced by condensation of metal atoms in an inert-gas stream. For the cases of both alkali [1,2] and transition metals [3], mass spectra of ionized clusters show several large peaks at "magic" mass numbers, providing evidence for an electronic shell organization of the electron states within a small metal cluster. Photoionization studies of unsupported potassium clusters [4] and copper anion clusters [5] exhibit evidence of this shell structure.

These measurements on gas-phase or unsupported clusters provide no information on the quantum electron states of a metal cluster deposited onto a substrate. This is a question of considerable interest, since supported metal clusters are important in a wide variety of electronic and chemical applications. Samples of metal clusters deposited on flat substrates in ultrahigh vacuum (UHV) have been studied by photoelectron spectroscopy [6-8]. Unfortunately, this technique does not have the sensitivity to explore the properties of an individual cluster and thus the experimental measurement is always a convolution over a distribution of cluster sizes. Recent scanning-tunneling-spectroscopy studies of a single Si<sup>10</sup> cluster have addressed this issue and have shown that information about the energy gap of a supported silicon cluster can be observed [9]. In this Letter, we show that a measurement of the energy distribution of electrons field emitted from an individual nanometer-size Au cluster reveals the quantized electronic structure of that cluster while supported on a conducting substrate. Prior studies on the size-dependent melting temperature of nanometer-size clusters [10,11] laid the groundwork for this research.

The nanometer-size Au clusters studied are produced using a multiple-expansion cluster source [10-12]. This source is capable of producing clusters with a controllable mean size and a narrow size distribution as described previously [12]. In our experiment, the size distribution of the cluster beam was determined from transmission-electron micrographs which revealed a narrow size distribution with a most probable diameter of  $1.0 \pm 0.2$  nm. The results described below were obtained from one such

cluster deposited on a W(110) substrate.

The ability to resolve the electronic structure of an individual cluster results from the point-projection magnification inherent in any field-emission experiment. By depositing nanometer-size clusters on the apex of a sharp field emitter, magnifications of  $\sim 10^6$  are readily obtained. In our experiments, a tungsten field-emission tip was prepared and mounted in an UHV-compatible transfer cell. The transfer cell, which has been described elsewhere [10], can transport cluster samples from the cluster-beam apparatus to a UHV field-emission apparatus without exposure to ambient conditions.

The sample cluster was obtained as follows. A clean W(110) tip was inserted into the cluster beam until the deposition of an individual cluster was detected. By reducing the voltage on the tip to about  $\frac{1}{2}$  to  $\frac{2}{3}$  of its original value, the arrival of a single cluster on the field emitter can be determined by the appearance of a bright dot observed on a nearby fluorescent screen. This dot is the result of electrons field emitted from an individual cluster. After a single cluster was successfully captured on the apex of the W tip, the tip and its cluster were transferred to the energy-analyzer apparatus operating at a pressure of  $\sim 1.3 \times 10^{-8}$  Pa ( $\sim 1 \times 10^{-10}$  Torr).

Inside the energy analyzer, electrons emitted from the cluster are observed on a fluorescent screen (see Fig. 1) and steered into the entrance slit of an electron energy analyzer using either electrostatic or magnetic deflection techniques. The energy analyzer is composed of a retardation analyzer and a 127° differential analyzer as described elsewhere [13,14] and has a resolution of  $\sim 70$  meV [15]. The energy analyzer is shielded by high-permeability Mumetal to screen stray magnetic fields. During a measurement of the energy distribution of electrons from the cluster, the total emission current was limited to 0.5 nA or less. At these emission currents, no single-electron charging effects were observed [16,17]. This implies that the RC time constant of the supported cluster was less than the average time between electron emission and indicates that the effective resistance  $R$  between the cluster and substrate must be less than  $\sim 6 \times 10^9 \Omega$ .

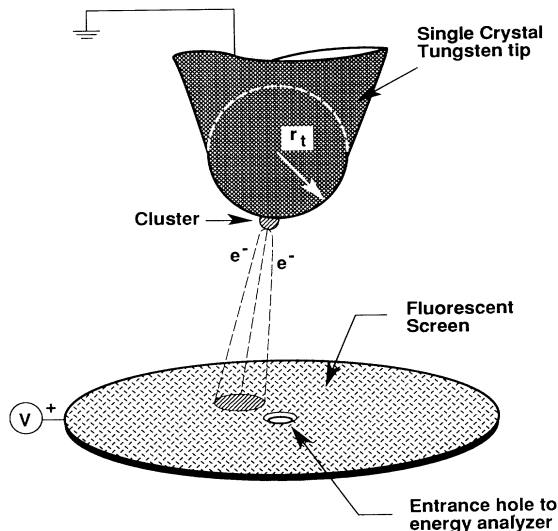


FIG. 1. Schematic diagram showing a cluster supported on a tungsten field-emission tip. Because of the high radius of curvature of the cluster with respect to the field-emission tip, electrons field emitted from the cluster can be readily identified on the fluorescent screen.

Generally, the field-emission energy spectrum is expected to exhibit two distinct distributions—one due to the contribution of electrons emitted from the underlying substrate and the other from the cluster itself (see Fig. 2). The relative height and position of the cluster contribution is related to the degree of coupling of the cluster to the substrate.

The energy distribution observed from the nominal 1-nm-diam Au cluster supported on W(110) is shown in Fig. 3(a). The data are plotted as a function of the energy of emitted electrons, with the zero of energy defined as the Fermi level ( $E_F$ ) of the substrate. In this experiment,  $E_F$  was accurately determined by thermally desorbing the cluster from the tip and measuring the energy distribution from the underlying W tip [see Fig. 3(b)]. The distribution from the substrate was analyzed by the established theory of field emission [18] and used to determine both  $E_F$  and the work function of the substrate. This procedure showed that the cluster states are shifted  $\sim 2.5$  eV below  $E_F$  of the substrate.

A number of distinct peaks, which mirror the quantized density of states of the supported cluster, are also evident in Fig. 3(a). A characteristic of the measured electron energy distribution is the sensitivity of these individual peak heights to the applied electric field, indicating a resonant enhancement of the tunneling current. The applied field also controls the position in energy of the observed peaks. By contrast, the electrons emitted from the substrate [Fig. 3(b)] show no shift with field. Careful studies also revealed no emission from states at energies near  $E_F$  of the substrate when the cluster was present, even though counting intervals extending up to a 5-min

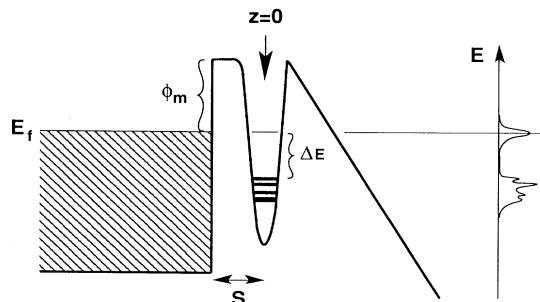


FIG. 2. A potential barrier diagram showing the Fermi level of the substrate, the quantized energy states of the cluster, and the deformed potential barrier due to the applied electric field. The distribution of electrons emitted from the cluster is also shown schematically.

dwelt time per channel were employed.

The structure in the energy distribution reported in Fig. 3(a) was reproduced many times over a period of a few weeks. However, other clusters studied with the same nominal size did not necessarily show the same structure, indicating the important role played by the electronic coupling between the cluster and the substrate. Similar variations in electronic structure have also been reported for Si clusters supported on Au substrates [9]. A study of different-size Au clusters supported on W tips

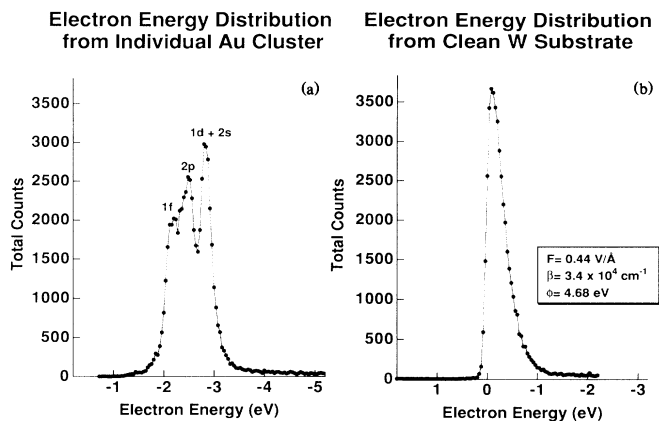


FIG. 3. (a) The field-emission spectrum observed with an applied voltage of 2550 V from a Au cluster of  $\sim 1$  nm diam. The electron energy distribution is dominated by three prominent peaks that are related to the electronic structure of the gold cluster. The labels identify the tentative origin of the peaks based on the electron shell-model calculation discussed in the text. (b) The electron energy distribution from the clean tungsten substrate after the cluster is removed by flashing the tip to white heat. This distribution allows an identification of the substrate  $E_F$  which is taken as the zero of energy. The field strength at the W substrate is related to the applied voltage by  $F = \beta V$ . The parameter  $\beta$  and the substrate work function  $\phi_s$  can be determined from a Fowler-Nordheim analysis of field-emission data.

indicates that the cluster's energy distribution shifts toward the substrate  $E_F$  with increasing size, with all structure disappearing for clusters with diameters greater than  $\sim 3$  nm [19].

It remains to identify the electronic states responsible for the observed structure in the cluster field-emission spectrum. In this context, it is useful to apply a modified resonance-tunneling theory developed for a single atom adsorbed on a field-emission tip by Gadzuk [20]. If the  $6s$  electrons of the gold atoms comprising the cluster are decoupled from their atoms and free to move under the influence of a spherical harmonic potential [21] specified by

$$V(r) = -V_0 + \frac{1}{2} M_e \omega^2 r^2, \quad (1)$$

then the energy spectrum of these electrons is discrete and the eigenstates for the harmonic part of the potential are defined by [22]

$$|c_0\rangle = A_{nlm} r^l e^{-\lambda r^2/2} {}_1F_1(-n; l + \frac{3}{2}; \lambda r^2) Y_{l,m}(\theta, \phi), \quad (2)$$

where  $\lambda = M_e \omega / \hbar$ , and  ${}_1F_1$  is a hypergeometric series that is a function of the principal quantum number  $n$  and the angular momentum  $l$ . The energy shift is given by

$$\Delta E \approx \langle c_0 | eV_{fp} | c_0 \rangle + \phi_{s-c}, \quad (3)$$

where  $V_{fp}$  describes the field penetration of the electric field into the cluster and  $\phi_{s-c}$  is the work-function difference between the substrate and the Au cluster. This latter quantity can be estimated by (i) measuring the work function of the W substrate using standard Fowler-Nordheim techniques [18] and (ii) relying on estimates of the size-dependent work function of supported Au clusters determined by Castro *et al.* [23].

In order to evaluate Eq. (3), the effects of field penetration were estimated in the following way. If a metal sphere is placed in a uniform external electric field ( $\mathbf{E}_0 = -E_0 \hat{z}$ ), the magnitude of the field on the spherical surface with radius  $R$  is given classically by

$$E(R) = -3E_0 \cos\theta. \quad (4)$$

Under steady-state conditions, the induced charge density on the cluster can be related to the electric field by [24]

$$\nabla \rho(r) = (\sigma/D) E(r), \quad (5)$$

where  $\sigma$  is the conductivity and  $D$  is a diffusion constant for charge in the cluster. Using Gauss's law and the boundary condition specified by Eq. (4),  $\rho(r)$  can be eliminated from Eq. (5), yielding the electric field within the cluster:

$$E(r) \approx \frac{C \cos\theta}{r} [e^{r/\lambda_D} - e^{-r/\lambda_D}], \quad (6)$$

with  $C = -3RE_0/[e^{R/\lambda_D} - e^{-R/\lambda_D}]$ . In this model  $\lambda_D$ , the Debye wavelength, equals  $\epsilon D/\sigma$  and is equivalent to the Thomas-Fermi screening length in a free-electron approximation. For bulk Au,  $\lambda_D \sim 0.06$  nm. Since  $E(r)$  is

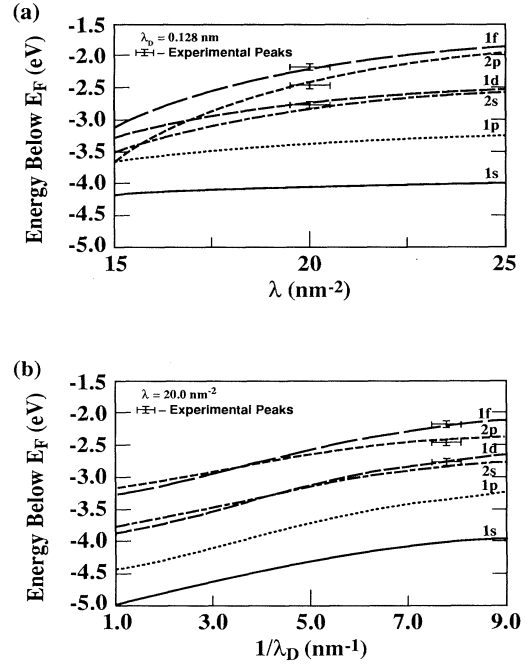


FIG. 4. The shift in the position of the energy levels of the shell model as a function of (a)  $\lambda$  and (b)  $\lambda_D$ . The position of the experimental features measured from Fig. 3(a) are shown. The parameters used in this calculation are cluster radius  $r_c = 0.54$  nm,  $\phi(\text{cluster}) = 5.7$  eV,  $\phi(\text{substrate}) = 4.68$  eV, distance between substrate and cluster  $= 0.5$  nm. The best values for the two parameters are  $\lambda = 20$  nm $^{-2}$  and  $\lambda_D = 0.128$  nm.

parallel to  $z$  inside the cluster, the induced potential due to field penetration is given by

$$V_{fp} \approx -\frac{C \lambda_D^2}{r^2} \left[ \frac{2r}{\lambda_D} \cosh(r/\lambda_D) - 2 \sinh(r/\lambda_D) \right]. \quad (7)$$

This result can be used in Eq. (3) to estimate the field-dependent energy shift for the various shell states ( $n, l$ ) of the cluster. The two parameters,  $\lambda$  and  $\lambda_D$ , were iteratively adjusted until the shift of the shell states were in alignment with the observed peak positions in the measured energy distribution shown in Fig. 3(a). The results of this procedure are summarized in Fig. 4 for different shell levels of the cluster. Good enough agreement between the position of the peaks and the estimates of this model are found to allow a tentative identification of the electronic states responsible for the structure observed [see labels in Fig. 3(a)]. In addition to the energy shift, a lifetime broadening and a resonance-tunneling factor can also be estimated for each feature. These factors control the width of the structure as well as the relative height of the peaks observed but are difficult to calculate exactly.

In summary, the field-emission energy distribution from a single supported nanometer-size Au cluster has been measured and found to contain significant structure, providing good evidence of quantized electronic states in

an individual 1-nm-diam Au cluster that survive when the cluster is supported on a W(110) surface. Using the electron shell model, a reasonable account for the experimental observations is obtained and a tentative identification of the shell levels responsible for the observed structure is proposed.

The authors would like to express their thanks to E. Galvão da Silva for useful comments on the manuscript. This work was partially supported by the U.S. Department of Energy under Grant No. DE-FG02-88ER45162 and by the National Science Foundation under Grant No. CBT-8722348.

- 
- [1] W. D. Knight, K. Clemenger, W. A. de Heer, W. A. Saunders, M. Y. Chou, and M. L. Cohen, *Phys. Rev. Lett.* **52**, 2141 (1984).
  - [2] S. Bjørnholm, J. Borggreen, O. Echt, K. Hansen, J. Pedersen, and H. D. Rasmussen, *Phys. Rev. Lett.* **65**, 1627 (1990).
  - [3] I. Katakuse, T. Ichihara, Y. Fujita, T. Matsuo, T. Sakurai, and H. Tsuda, *Int. J. Mass Spectrom. Ion Processes* **67**, 229 (1985).
  - [4] W. A. Saunders, K. Clemenger, W. A. de Heer, and W. D. Knight, *Phys. Rev. B* **32**, 1366 (1985).
  - [5] C. L. Pettiette, S. H. Yang, M. J. Craycraft, J. Conceicao, R. T. Laaksonen, O. Cheshnovsky, and R. E. Smalley, *J. Chem. Phys.* **88**, 5377 (1988).
  - [6] S. T. Lee, G. Apai, M. G. Mason, R. Benbow, and Z. Hurych, *Phys. Rev. B* **23**, 505 (1981).
  - [7] M. G. Mason, *Phys. Rev. B* **27**, 748 (1983).
  - [8] S. B. Diczienzo and G. K. Wertheim, *Comments Solid State Phys.* **11**, 203 (1985).
  - [9] Y. Kuk, M. F. Jarrold, P. J. Silverman, J. E. Bower, and W. L. Brown, *Phys. Rev. B* **39**, 11168 (1989).
  - [10] T. Castro, R. Reifengerger, E. Choi, and R. P. Andres, *Surf. Sci.* **234**, 43 (1990).
  - [11] T. Castro, R. Reifengerger, E. Choi, and R. P. Andres, *Phys. Rev. B* **42**, 8548 (1990).
  - [12] E. Choi and R. P. Andres, in *Physics and Chemistry of Small Clusters*, edited by P. Jena, B. K. Rao, and S. N. Khanna (Plenum, New York, 1987), p. 61.
  - [13] D. L. Haavig and R. Reifengerger, *Surf. Sci.* **151**, 128 (1985).
  - [14] C. M. Egert and R. Reifengerger, *Surf. Sci.* **145**, 159 (1984).
  - [15] Y. Gao, R. Reifengerger, and R. M. Kramer, *J. Phys. E* **18**, 381 (1985).
  - [16] J. B. Barner and S. T. Ruggiero, *Phys. Rev. Lett.* **59**, 807 (1987).
  - [17] R. Wilkins, E. Ben-Jacob, and R. C. Jaklevic, *Phys. Rev. Lett.* **63**, 801 (1989).
  - [18] J. W. Gadzuk and E. W. Plummer, *Rev. Mod. Phys.* **43**, 487 (1973).
  - [19] M. E. Lin, R. P. Andres, and R. Reifengerger (to be published).
  - [20] J. W. Gadzuk, *Phys. Rev. B* **1**, 2110 (1970).
  - [21] The harmonic potential is chosen for this analysis because the wave functions for this model allow a straightforward evaluation of the relevant matrix elements.
  - [22] J. M. Eisenberg and W. Greiner, *Nuclear Theory* (North-Holland, Amsterdam, 1970), Vol. 1.
  - [23] T. Castro, Y. Z. Li, R. Reifengerger, E. Choi, S. B. Park, and R. P. Andres, *J. Vac. Sci. Technol. A* **7**, 2845 (1989).
  - [24] Neil W. Ashcroft and N. David Mermin, *Solid State Physics* (Holt, Rinehart and Winston, New York, 1976).